An International Journal of Optimization and Control: Theories & Applications
ISSN: 2146-0957 eISSN: 2146-5703
Vol.15, No.3, pp.449-463 (2025)
https://doi.org/10.36922/IJOCTA025060018

RESEARCH ARTICLE

Computational aspects of the crop field segmentation problem based on anisotropic active contour model

Ciro D'Apice[1], Umberto De Maio[2], Peter I. Kogut[3,4], and Rosanna Manzo[5*]

[1]Department of Management Innovation Systems, University of Salerno, Fisciano, Italy
[2]Department of Mathematics and Applications "R. Caccioppoli", University of Naples "Federico II", Naples, Italy
[3]Department of Differential Equations, Oles Honchar Dnipro National University, Dnipro, Ukraine
[4]EOS Data Analytics Ukraine, Dnipro, Ukraine
[5]Department of Political and Communication Sciences, University of Salerno, Fisciano, Italy
cdapice@unisa.it, udemaio@unina.it, p.kogut@i.ua, peter.kogut@eosda.com, rmanzo@unisa.it

ARTICLE INFO

Article History:
Received: February 4, 2025
1st revised: February 11, 2025
2nd revised: April 4, 2025
Accepted: April 11, 2025
Published Online: May 20, 2025

Keywords:
Segmentation problem
Piecewise smooth approximation
Optimality conditions
Active contour model
Euler-Lagrange equation

AMS Classification 2010:
26A33; 34A08; 35H15; 34K50

ABSTRACT

In this paper, we analyze the numerical aspects of the practical implementation of the generalized active contour model, that has been recently proposed in the literature, for extracting agricultural crop fields with a high level of inhomogeneity from satellite data. We also derive the corresponding Euler–Lagrange equation and discuss its relaxation method.

1. Introduction

This paper deals with the numerical aspects of the implementation of the generalized active contour model, which has been recently proposed in,[1] for extracting agricultural crop fields with a high level of inhomogeneity from satellite data. These investigations have been justified by various applications, such as in satellite image segmentation under remote sensing of the Earth's surface. Fixed a field $\Omega \subset \mathbb{R}^2$, one of the fundamental problems in agriculture is to give a disjunctive decomposition into a finite quantity of nonempty subsets $\Omega = \Omega_1 \cup \Omega_2 \cup \cdots \cup \Omega_K \cup \Omega^*$ such that a distinctive value of some agricultural index (PVI, NDVI, LAI, etc.) could be associated to each of these subsets. The characteristic feature of the decomposition is that it has to be closely related to a given objective agricultural index $f : \Omega \to \mathbb{R}$. Namely, this decomposition has to inherit the following properties:

(a) $\{\Omega_i\}_{i=1}^K$ are open subsets of Ω with nonempty interior, whereas Ω^* stands for the boundaries between different Ω_j;
(b) within each Ω_i the objective agricultural index f varies smoothly and/or slowly;
(c) the function f cannot vary discontinuously inside each Ω_i;
(d) the decomposition is optimal in the following sense: the approximation of f by a piece-wise constant function $f^* : \Omega \to \mathbb{R}$ is such that the restrictions f^* to the pieces

*Corresponding Author

$\Omega_j,\ f^*|_{\Omega_j}$, are defined as

$$|f^*|_{\Omega_j}(x) = \langle f\rangle_{\Omega_j} := \frac{1}{|\Omega_j|}\int_{\Omega_j} f(s)\,ds, \quad \forall\, j = 1,\dots,K, \forall\, x \in \Omega_j,$$

and the 1-D Hausdorff measure of the set $\bigcup_{j=1}^{K} \partial\Omega_j$ should be as small as possible.

Hereinafter, the decomposition of Ω satisfying properties (a)–(d) is denoted with f-decomposition.

The role of the function $f : \Omega \to \mathbb{R}$ is explained by pointing out that after the f-decomposition the new objects $\{\Omega_j\}_{j=1}^{K}$ should have homogeneous values of f (see[2,3]). To characterize a measure of the variability of f in each subdomain Ω_j, one can calculate the coefficient of variation, that is, it is the ratio of the standard deviation of $f(x)$ within Ω_j to its mean $\langle f\rangle_{\Omega_j}$. Furthermore, if we consider applications in agriculture it might be reasonable to regard the NDVI-characteristic as the primary feature of the zone of interest Ω, that is, in this case, $f(x) = \mathrm{NDVI}(x)$ for all $x \in \Omega$. However, a thorough analysis of this issue shows that it is a difficult task to understand NDVI characteristics quantitatively over Ω. By presuming that the vegetation data generated from the NDVI is uniformly and smoothly distributed within the specific crop fields, numerous studies have restricted this interpretation.[4,5] If they attempt to use the NDVI on heterogeneous canopies, for example, plantations that have weeds, mixed soil, and various crop mixtures where the vegetation has varying NDVI characteristics because of spatial variability, this assumption is violated.

Accordingly, the data acquired in this manner is a valuable source of information that may be applied to the management of environmental resources.[6,7] Specifically, it enables us to determine the crop's health and find out whether there are trouble spots within the designated fields or areas where the crops require nutrients or water. A similar point of view is recommended as crucial in.[3,6] Some methods for assessing such characteristics have recently been proposed in.[8–10] The most stringent barrier to creating such a decomposition, however, is that these subdomains cannot include even minor portions of various fields with plausibly distinct crops, nor should they overlap or contain any fragments of field borders. Because of this, the segmentation challenge indicated above is fairly difficult.

Moreover, the principal distinguishing characteristic of f-decomposition is the impossibility to reduce it to the well-known settings of the segmentation problem (consult the model of Mumford-Shah[11] or the approaches proposed by[12–19] along with the others). We refer to the recent study[17] for an overview of the state of the art in this topic.

To sort out these issues, we involve an anisotropic specification of the standard active contour model. Apparently, the latter was first introduced in[20] to transform the image segmentation problem into a minimization problem in a suitable functional space, and it offered a fresh perspective on image segmentation, which was referred to as the focus and hot spot of analysis in.[21] The subject of image segmentation has seen the proposal of numerous good algorithms based on active contour models in recent years (we recommend that readers consult the latest publications[22–28] and the bibliography therein). However, their correct application to the NDVI-decomposition of agricultural fields remains an open problem nowadays.

The main idea, that was realized in the new setting of variational issue for the f-decomposition, is that we associate with a given objective function $f : \Omega \to \mathbb{R}$ the constrained optimization problem as follows:

$$J(c,\varphi) = T(c,\varphi) + \alpha\sum_{j=1}^{m}\int_{\Omega} |M^f D\chi_{\{\varphi(x)>l_j\}}| \to \inf_{\varphi\in\Xi}, \quad (1)$$

where $T : \mathbb{R}^{m+1} \times BV(\Omega) \to \mathbb{R}$ is a fidelity term, $\{l_0, l_1, \dots, l_{m+1}\}$ is a given collection of distinct level values, $\chi_{\{\varphi(x)>l_j\}}$ is the characteristic function of the set $\{x \in \Omega : \varphi(x) > l_j\}$, and the set of feasible solutions Ξ is defined as follows: $(c,\varphi) \in \Xi$ if and only if $(c,\varphi) \in \mathbb{R}^{m+1} \times BV(\Omega)$ and

$$l_0 \le \varphi(x) \le l_{m+1} \text{ a.e. in } \Omega,$$
$$c = (c_0, c_1, \dots, c_m),\ c_j \ge 0,\ j = 0,\dots,m.$$

As for the matrix-value function $M^f(\cdot) : \Omega \to \mathbb{R}^{2\times 2}$, it is the so-called anisotropic diffusion tensor that avoids the emergence of subdomains with f discontinuity zones or locations where this function has a tendency to change quickly.

Thus, the main idea, which we push forward, is that the segmentation problem should be given as a constrained minimization problem with a special anisotropic cost functional, where the "effect of anisotropy" we associate with the structure topology of f-distribution (see[29]). With that in mind, we utilize the main characteristic of the given function f — the normal unit vector field $\theta : \Omega \to \mathbb{R}^2$ to level sets of f. As a result,

we define $M^f(\cdot)$ as a parametrized square matrix function $M^f(x) = \left[I - \eta^2 \theta(x) \otimes \theta(x)\right]$ and demonstrate that the f-decomposition of the domain Ω relies heavily on this tensor (the technical details are explained in Section 2). As for the fidelity term $T(c, \varphi)$, we give its precise definition in Section 2. Its characteristic feature is the fact that instead of the standard Euclidean metric, we involve into consideration the Jeffrey divergency as a more stable metric with respect to outliers.

The outcomes of simulations using satellite photos of agricultural fields, where the area of high oscillatory edges (the crop locations' boundaries) is rather significant, support the advantage of including M^f in the final term of J_ε. We refer to Section 4 for further information.

Thus, if $(c^0, \varphi^0) \in \underset{(c,\varphi)\in\Xi}{\operatorname{Absmin}} J(c, \varphi)$, then

$$f^*|_{\Omega_j}(x) = c_j^0 := \frac{1}{|\Omega_j|} \int_{\Omega_j} f(s)\, ds, \quad \forall\, x \in \Omega_j, \quad \text{and} \quad \forall\, j = 0, \ldots, m.$$

is a piece-wise approximation of f and the corresponding f-decomposition takes the form

$$\begin{aligned}
\Omega_0 &= \left\{ x \in \Omega \,:\, \left(\varphi^0\right)_\rho (x) < l_1 \right\}, \\
\Omega_j &= \left\{ x \in \Omega \,:\, l_j < \left(\varphi^0\right)_\rho (x) < l_{j+1} \right\}, \\
& \quad j = 1, \ldots, m-1, \\
\Omega_m &= \left\{ x \in \Omega \,:\, \left(\varphi^0\right)_\rho (x) > l_m \right\}, \\
\Omega_* &= \bigcup_{j=1}^{m} \left\{ x \in \Omega \,:\, \left(\varphi^0\right)_\rho (x) = l_j \right\}.
\end{aligned}$$

Here, $\left(\varphi^0\right)_\rho \in C^\infty(\overline{\Omega})$ denotes a smooth approximation of $\varphi^0 \in BV(\Omega)$. Moreover, setting $\Omega = \Omega_i$, $i = 0, 1, \ldots, m$, while for a new pair of subdomains, the mean values of f continue to be distinct, we can iteratively carry on with the decomposition process.

The outline of the paper is as follows. In Section 2 we introduce the setting of the optimization problem for f-decomposition of Ω and discuss its main principle features. Section 3 is devoted to prove that, under some assumptions, the corresponding optimality system can be represented in the form of the Euler–Lagrange equation with the corresponding initial and boundary conditions. The aim of Section 4 is to describe the numerical scheme and a procedure to solve the Euler–Lagrange system numerically. Section 4 includes the outcomes of simulation using real-life satellite images, demonstrating that the proposed model exhibits accuracy and efficiency.

2. Statement of the piecewise-constant Mumford–Shah segmentation problem

Denote by Ω a bounded open subset of $\mathbb{R}^2$ with a Lipschitz boundary. Given a subset $E \subset \Omega$, let $|E|$ be its 2-dimensional Lebesgue measure $\mathcal{L}^2(E)$, $\overline{E}$ its closure, ∂E its boundary, and χ_E of E the characteristic function. The notation $u|_E$ denotes the restriction of a given function u to the set $E \subseteq \Omega$. Indicate the infinitely differentiable functions having compact support in Ω by $C_0^\infty(\Omega)$. Let $\mathcal{H}^k$ be the Hausdorff k-dimensional measure and $\mu \llcorner E$ the measure μ restricted to the set E.

Let $f : \Omega \to \mathbb{R}$ be a given objective function that can be interpreted as a gray-scale image such that a value $\gamma > 0$ exists satisfying

$$f(x) \geq \gamma > 0 \text{ a.e. in } \Omega, f \in L^\infty(\Omega). \tag{2}$$

The following statement for the f-decomposition of Ω in the framework of the Mumford–Shah segmentation problem has been recently proposed in[1]

$$\begin{aligned}
J(c, \varphi) = & \int_\Omega (f - c_0) \log\left(\frac{f}{c_0}\right) \chi_{\{\varphi(x) < l_1\}}\, dx \\
& + \sum_{j=1}^{m-1} \int_\Omega (f - c_j) \log\left(\frac{f}{c_j}\right) \\
& \qquad \times \left[\chi_{\{\varphi(x) > l_j\}} - \chi_{\{\varphi(x) > l_{j+1}\}}\right] dx \\
& + \int_\Omega (f - c_m) \log\left(\frac{f}{c_m}\right) \chi_{\{\varphi(x) > l_m\}}\, dx \\
& + \alpha \sum_{j=1}^{m} \int_\Omega |M^f D\chi_{\{\varphi(x) > l_j\}}| \to \inf_{\varphi \in \Xi},
\end{aligned} \tag{3}$$

where $\alpha > 0$ is a weight coefficient and feasible solutions are given by: $(c, \varphi) \in \Xi$ iff $(c, \varphi) \in \mathbb{R}^{m+1} \times BV(\Omega)$ and

$$\begin{aligned}
& l_0 \leq \varphi(x) \leq l_{m+1} \text{ a.e. in } \Omega, \\
& c = (c_0, c_1, \ldots, c_m),\ c_j \geq 0,\ j = 0, \ldots, m.
\end{aligned} \tag{4}$$

Here, $\{l_0, l_1, \ldots, l_{m+1}\}$ is a given collection of distinct level values, and $M^f(\cdot) \in C^\infty(\Omega; \mathbb{R}^{2\times 2})$ stands for the squared matrix such that

$$M^f(x) = \left[I - \eta^2 \theta(x) \otimes \theta(x)\right] \tag{5}$$

with

$$\theta(x) = \begin{cases} \nabla f_\sigma(x) |\nabla f_\sigma(x)|^{-1}, & \text{if } |\nabla f_\sigma(x)| \neq 0, \\ 0, & \text{otherwise,} \end{cases}$$

where the stated threshold, $\eta \in (0, 1)$, must be close enough to 1, $f_\sigma = \left(G_\sigma * f(\cdot)\right)(x) := \int_\Omega f(y) G_\sigma(x - y)\, dy$ is the convolution of f with

a Gaussian kernel, and

$$G_\sigma(x) = \frac{1}{\left(\sqrt{2\pi}\sigma\right)^2} \exp\left(-\frac{|x|^2}{2\sigma^2}\right), \quad \sigma > 0,$$

and $\sigma > 0$ is a tuned small positive value.

For the simplicity, we assume that the vector field $\theta \in C^\infty(\Omega;\mathbb{R}^2)$ vanishes along the boundary $\partial\Omega$, that is,

$$M^f(x) = I \quad \forall\, x \in \partial\Omega. \tag{6}$$

As for the total variation of the measure $M^f Du$, we define it by the rule

$$\begin{aligned} |M^f Du|(\Omega) &:= \int_\Omega |M^f Du| \\ &= \sup\Big\{ \int_\Omega u \operatorname{div}(M^f\varphi)\, dx \ : \ \varphi \in C_0^1(\Omega;\mathbb{R}^2), \\ &\qquad |\varphi(x)| \le 1 \ \forall\, x \in \Omega)\Big\}. \end{aligned} \tag{7}$$

Since the existence of minimizers to the problem (3)–(4) remains an open issue nowadays, according to,[1] the following family of two-parametric approximated problems should be used

$$\begin{aligned} J_{\varepsilon,\tau}(c,\varphi) &= \int_\Omega (f-c_0)\log\left(\frac{f}{c_0}\right)\left[\chi_{A_0^\tau}\right]_\varepsilon dx + \\ &\sum_{j=1}^{m-1}\int_\Omega (f-c_j)\log\left(\frac{f}{c_j}\right)\left(\left[\chi_{A_j^\tau}\right]_\varepsilon - \left[\chi_{A_{j+1}^\tau}\right]_\varepsilon\right) dx \\ &+ \int_\Omega (f-c_m)\log\left(\frac{f}{c_m}\right)\left[\chi_{A_m^\tau}\right]_\varepsilon dx \\ &+ \frac{1}{\varepsilon}\left[\|\Psi(l_0-\varphi)\|_{L^1(\Omega)} + \|\Psi(\varphi-l_{m+1})\|_{L^1(\Omega)}\right] \\ &+ \varepsilon|M_\varepsilon^f D\varphi|(\Omega) \\ &+ \alpha\sum_{j=1}^m \int_{\Omega_{2\varepsilon}} \left|M_\varepsilon^f D\left[\chi_{E_j^\tau}\right]_\varepsilon\right| \to \inf_{\varphi\in\Xi_\varepsilon}, \end{aligned} \tag{8}$$

where τ and ε are small parameters, which vary within strictly decreasing sequences of positive numbers converging to 0,

$$\left.\begin{aligned} A_0^\tau &= \{x\in\Omega : \varphi(x) \le l_1 - \tau\}, \\ A_j^\tau &= \{x\in\Omega : \varphi(x) \ge l_j + \tau\}, \\ E_j^\tau &= \{x\in\Omega : \varphi(x) \ge l_j - \tau\}, \\ j &= 1,\dots,m, \end{aligned}\right\} \tag{9}$$

$$\begin{aligned} \Omega_{2\varepsilon} &= \left\{x\in\mathbb{R}^2 : \operatorname{dist}(x,\Omega) \le 2\varepsilon\right\}, \\ M_\varepsilon^f(x) &= \left[I - (1-\varepsilon)^2\theta(x)\otimes\theta(x)\right], \end{aligned} \tag{10}$$

$$\Psi(z) = \left\{\begin{array}{ll} z^{2-\tau}, & \text{if } z \ge 0, \\ 0, & \text{if } z < 0, \end{array}\right\} \tag{11}$$

with a given exponent $\delta \in (1,2)$, and

$$\begin{aligned} \Xi_\varepsilon = \big\{&(c,\varphi) \in \mathbb{R}^{m+1}\times BV(\Omega) \ : \\ &c = (c_0,c_1,\dots,c_m),\ c_j \ge 0,\ j = 0,\dots,m\big\}. \end{aligned} \tag{12}$$

As for the functions $\left[\chi_{A_j^\tau}\right]_\varepsilon(\cdot), \left[\chi_{E_j^\tau}\right]_\varepsilon(\cdot) \in C^\infty(\mathbb{R})$, they have the following representations:

$$\begin{aligned} \left[\chi_{A_0^\tau}\right]_\varepsilon &= H_\varepsilon(l_1 - \tau - \varphi), \\ \left[\chi_{A_j^\tau}\right]_\varepsilon &= H_\varepsilon(\varphi - l_j - \tau),\ j = 1,\dots.m, \\ \left[\chi_{E_j^\tau}\right]_\varepsilon &= H_\varepsilon(\varphi - l_j + \tau),\ j = 1,\dots.m, \end{aligned}$$

where $H_\varepsilon(z) = [\eta_\varepsilon * H](z)$ stands for the smooth approximation of the Heaviside step function $H(z) = \left\{\begin{smallmatrix} 1,\ z\ge 0 \\ 0, z<0\end{smallmatrix}\right\}$ through the mollification. For the practical implementations, it would be enough to set

$$H_\varepsilon(z) = \left\{\begin{array}{ll} 0, & z < -\varepsilon, \\ \frac{z}{2\varepsilon} + \frac{1}{2}\left(1 + \frac{1}{\pi}\sin\frac{\pi z}{\varepsilon}\right), & -\varepsilon \le z \le \varepsilon, \\ 1, & z > \varepsilon. \end{array}\right. \tag{13}$$

Considering that the slope of $H_\varepsilon(z)$ is sufficiently near to $H(z)$, the Heaviside function for $\varepsilon > 0$ small enough, and that

$$\begin{aligned} &H_\varepsilon(\cdot) \in C^2_{loc}(\mathbb{R}), \\ &\|H(\cdot) - H_\varepsilon(\cdot)\|_{L^1(\mathbb{R})} = \varepsilon, \quad \forall\, \varepsilon > 0, \end{aligned} \tag{14}$$

the function $H_\varepsilon(\cdot)$ is seen as a $H(z)$ pointwise approximation.

The function $\delta_\varepsilon \in C_0^1(\mathbb{R})$ is defined, establishing

$$\begin{aligned} \delta_{1,\varepsilon}(z) &= \frac{dH_\varepsilon(z)}{dz} \\ &= \left\{\begin{array}{ll} 0, & |z| > \varepsilon, \\ \frac{1}{2\varepsilon}\left(1 + \cos\frac{\pi z}{\varepsilon}\right), & |z| \le \varepsilon, \end{array}\right. \quad \forall\, z \in \mathbb{R}, \end{aligned} \tag{15}$$

as an approximation of $\delta(z)$, that is, the Dirac function.

The following result has recently been established in:[1]

Theorem 1. *Let $f : \Omega \to \mathbb{R}$ be a given grayscale image satisfying properties* (2)*. Then, for each $\varepsilon \in (0,1)$ and $\tau > 0$ small enough, the constrained minimization problem* (8)–(12) *admits at least one solution. Moreover, if $(c^0_{\varepsilon,\tau}, \varphi^0_{\varepsilon,\tau}) \in \Xi_\varepsilon$ is a local minimizer to problem* (8)–(12)*, then*

$$c^0_{\varepsilon,\tau,0} = c_0(\varphi^0_{\varepsilon,\tau}) = \frac{\int_\Omega f H_\varepsilon(l_1 - \varphi^0_{\varepsilon,\tau} - \tau)\, dx}{\int_\Omega H_\varepsilon(l_1 - \varphi^0_{\varepsilon,\tau} - \tau)\, dx},$$

$$c^0_{\varepsilon,\tau,j} = c_j(\varphi^0_{\varepsilon,\tau}) = \frac{\int_\Omega f\left[H_\varepsilon(\varphi^0_{\varepsilon,\tau} - l_j - \tau) - H_\varepsilon(\varphi^0_{\varepsilon,\tau} - l_{j+1} - \tau)\right] dx}{\int_\Omega \left[H_\varepsilon(\varphi^0_{\varepsilon,\tau} - l_j - \tau) - H_\varepsilon(\varphi^0_{\varepsilon,\tau} - l_{j+1} - \tau)\right] dx},$$

$$c^0_{\varepsilon,\tau,m} = c_m(\varphi^0_{\varepsilon,\tau}) = \frac{\int_\Omega f H_\varepsilon(\varphi^0_{\varepsilon,\tau} - l_m - \tau)\,dx}{\int_\Omega H_\varepsilon(\varphi^0_{\varepsilon,\tau} - l_m - \tau)\,dx}, \tag{16}$$

and the pair $\varphi^0_{\varepsilon,\tau}$ *satisfies the following optimality condition*

$$\begin{aligned}
&-\int_\Omega \left(f - c^0_{\varepsilon,\tau,0}\right)\log\left(\frac{f}{c^0_{\varepsilon,\tau,0}}\right)\\
&\qquad\times \delta_\varepsilon(l_1 - \varphi^0_{\varepsilon,\tau} - \tau)[\varphi - \varphi^0_{\varepsilon,\tau}]\,dx\\
&\quad+\sum_{j=1}^{m-1}\int_\Omega \left(f - c^0_{\varepsilon,\tau,j}\right)\log\left(\frac{f}{c^0_{\varepsilon,\tau,j}}\right)\\
&\qquad\times \delta_\varepsilon(\varphi^0_{\varepsilon,\tau} - l_j - \tau)\\
&\qquad\times H_\varepsilon(-\varphi^0_{\varepsilon,\tau} + l_{j+1} + \tau)[\varphi - \varphi^0_{\varepsilon,\tau}]\,dx\\
&\quad-\sum_{j=1}^{m-1}\int_\Omega \left(f - c^0_{\varepsilon,\tau,j}\right)\log\left(\frac{f}{c^0_{\varepsilon,\tau,j}}\right)\\
&\qquad\times \delta_\varepsilon(-\varphi^0_{\varepsilon,\tau} + l_{j+1} + \tau)\\
&\qquad\times H_\varepsilon(\varphi^0_{\varepsilon,\tau} - l_j - \tau)[\varphi - \varphi^0_{\varepsilon,\tau}]\,dx\\
&\quad+\int_\Omega \left(f - c^0_{\varepsilon,\tau,m}\right)\log\left(\frac{f}{c^0_{\varepsilon,\tau,m}}\right)\\
&\qquad\times \delta_\varepsilon(\varphi^0_{\varepsilon,\tau} - l_m - \tau)[\varphi - \varphi^0_{\varepsilon,\tau}]\,dx\\
&\quad+\frac{1}{\varepsilon}\int_\Omega \left[\Psi'(\varphi^0_{\varepsilon,\tau} - l_{m+1}) - \Psi'(l_0 - \varphi^0_{\varepsilon,\tau})\right]\\
&\qquad\times [\varphi - \varphi^0_{\varepsilon,\tau}]\,dx\\
&\quad+ j_{\varepsilon,\tau}(\varphi) - j_{\varepsilon,\tau}\left(\varphi^0_{\varepsilon,\tau}\right) \geq 0, \quad \forall\,\varphi \in BV(\Omega),
\end{aligned} \tag{17}$$

where

$$\begin{aligned}
\Phi_\varepsilon(\varphi) &= \frac{1}{\varepsilon}\left[\|\Psi(l_0 - \varphi)\|_{L^1(\Omega)}\right.\\
&\qquad\left.+\|\Psi(\varphi - l_{m+1})\|_{L^1(\Omega)}\right],\\
j_{\varepsilon,\tau}(\varphi) &= \varepsilon|M^f_\varepsilon D\varphi|(\Omega)\\
&\qquad+\alpha\sum_{j=1}^{m}\int_{\Omega_{2\varepsilon}}\left|M^f_\varepsilon D\left[\chi_{E^\tau_j}\right]_\varepsilon\right|.
\end{aligned}$$

Moreover, we have the following result concerning the asymptotic behavior of the approximated problem (8)–(12) (for the technical details, we refer to[30,31]).

Theorem 2. *Let* $\tau \ll 1$ *be a given positive value. Let* $\left\{(c^0_{\varepsilon,\tau}, \varphi^0_{\varepsilon,\tau}) \in \Xi_\varepsilon\right\}_{\varepsilon\to 0}$ *be a sequence of optimal pairs to the approximated minimization problems* (8)–(12). *Assume that* $\left\{\varphi^0_{\varepsilon,\tau}\right\}_{\varepsilon>0}$ *is a bounded sequence in* $BV(\Omega)$, *and the relaxed problem*

$$J_\tau(c,\varphi) \to \inf_{\substack{(c,\varphi)\in\Xi\\ \varphi\in BV(\Omega)}} \tag{18}$$

has a nonempty set of minimizers for the given value $\tau > 0$. *Then there exists a pair* $(c^*_\tau, \varphi^*_\tau) \in \Xi$ *such that* $\varphi^*_\tau \in BV(\Omega)$ *and, up to a subsequence,*

$$\begin{aligned}
c^0_{\varepsilon,\tau} &\to c^*_\tau \ \ \textit{in}\ \ \mathbb{R}^{m+1} \ \ \textit{as}\ \varepsilon\to 0,\\
\varphi^0_{\varepsilon,\tau} &\to \varphi^*_\tau \ \ \textit{strongly in}\ \ L^1(\Omega),\\
M^f D\varphi^0_{\varepsilon,\tau} &\overset{*}{\rightharpoonup} M^f D\varphi^*_\tau \ \textit{weakly-*}\ \textit{in}\ \ \mathcal{M}(\Omega;\mathbb{R}^2),\\
\inf_{(c,\varphi)\in\Xi} J_\tau(c,\varphi) &= J_\tau(c^*_\tau,\varphi^*_\tau)\\
&= \lim_{\varepsilon\to 0} J_{\varepsilon,\tau}(c^0_{\varepsilon,\tau},\varphi^0_{\varepsilon,\tau}) = \lim_{\varepsilon\to 0}\inf_{(c,\varphi)\in\Xi_\varepsilon} J_{\varepsilon,\tau}(c,\varphi),
\end{aligned}$$

where the objective functional $J_\tau : \Xi \to \mathbb{R}$ *is defined as*

$$\begin{aligned}
J_\tau(c,\varphi) &= \int_\Omega (f - c_0)\log\left(\frac{f}{c_0}\right)\chi_{A^\tau_0}\,dx\\
&\quad+\sum_{j=1}^{m-1}\int_\Omega (f - c_j)\log\left(\frac{f}{c_j}\right)\left[\chi_{A^\tau_j} - \chi_{A^\tau_{j+1}}\right]\,dx\\
&\quad+\int_\Omega (f - c_m)\log\left(\frac{f}{c_m}\right)\chi_{A^\tau_m}\,dx\\
&\quad+\alpha\sum_{j=1}^{m}\int_\Omega |M^f D\chi_{E^\tau_j}|.
\end{aligned}$$

3. On representation of optimality system (17) in the form of Euler–Lagrange equation

In this section, we characterize the solution $(c^0_{\varepsilon,\tau}, \varphi^0_{\varepsilon,\tau})$ of the minimization problem (8)–(12) for given values $\varepsilon \in (0,1)$ and $\tau > 0$ deriving for that the equation satisfied by $(c^0_{\varepsilon,\tau}, \varphi^0_{\varepsilon,\tau})$. To do so, we decompose $J_{\varepsilon,\tau} : \Xi_\varepsilon \to \mathbb{R}$ as the sum of three functionals, that is,

$$J_{\varepsilon,\tau}(c,\varphi) = I_{\varepsilon,\tau}(c,\varphi) + \Phi_\varepsilon(\varphi) + \Lambda_{\varepsilon,\tau}(\varphi), \tag{19}$$

where $I_{\varepsilon,\tau} : \mathbb{R}^{m+1} \times L^2(\Omega) \to \mathbb{R}$ and $\Phi_\varepsilon : L^2(\Omega) \to \mathbb{R}$ are defined by the rules

$$\begin{aligned}
I_{\varepsilon,\tau}(c,\varphi) &= \int_\Omega (f - c_0)\log\left(\frac{f}{c_0}\right)\left[\chi_{A^\tau_0}\right]_\varepsilon\,dx\\
&\quad+\sum_{j=1}^{m-1}\int_\Omega (f - c_j)\log\left(\frac{f}{c_j}\right)\\
&\qquad\times\left(\left[\chi_{A^\tau_j}\right]_\varepsilon - \left[\chi_{A^\tau_{j+1}}\right]_\varepsilon\right)\,dx\\
&\quad+\int_\Omega (f - c_m)\log\left(\frac{f}{c_m}\right)\left[\chi_{A^\tau_m}\right]_\varepsilon\,dx,
\end{aligned} \tag{20}$$

$$\begin{aligned}
\Phi_\varepsilon(\varphi) &= \frac{1}{\varepsilon}\left[\|\Psi(l_0 - \varphi)\|_{L^1(\Omega)}\right.\\
&\qquad\left.+\|\Psi(\varphi - l_{m+1})\|_{L^1(\Omega)}\right],
\end{aligned} \tag{21}$$

and $\Lambda_{\varepsilon,\tau} : L^2(\Omega) \to \mathbb{R}$ is defined by

$$\begin{aligned}
\Lambda_{\varepsilon,\tau}(\varphi) &= \varepsilon|M^f_\varepsilon D\varphi|(\Omega)\\
&\quad+\alpha\sum_{j=1}^{m}\int_{\Omega_{2\varepsilon}}\left|M^f_\varepsilon D\left[\chi_{E^\tau_j}\right]_\varepsilon\right|,
\end{aligned} \tag{22}$$

if $\varphi \in BV(\Omega)$, and

$$\Lambda_{\varepsilon,\tau}(\varphi) = \infty, \text{ if } \varphi \in L^2(\Omega) \setminus BV(\Omega).$$

Taking into account the fact that $\Psi \in C^1_{loc}(\mathbb{R})$, it can be shown that

$$\Phi_\varepsilon\left(\varphi^0_{\varepsilon,\tau} + \lambda h\right) = \Phi_\varepsilon\left(\varphi^0_{\varepsilon,\tau}\right) + \lambda D_\varphi \Phi_\varepsilon\left(\varphi^0_{\varepsilon,\tau}\right)[h] + r(h,\lambda),$$

for any $h \in L^2(\Omega)$, where, as $\lambda \to 0, |r(h,\lambda)| = o(|\lambda|)$, and $D_\varphi\Phi_\varepsilon(\varphi^0_{\varepsilon,\tau}) : L^2(\Omega) \to \mathbb{R}$ is a linear continuous functional with the following representation:

$$D_\varphi \Phi_\varepsilon\left(\varphi^0_{\varepsilon,\tau}\right)[h] = \frac{1}{\varepsilon}\Big[- \int_\Omega \Psi'(l_0 - \varphi^0_{\varepsilon,\tau}) h\, dx + \int_\Omega \Psi'(\varphi^0_{\varepsilon,\tau} - l_{m+1}) h\, dx\Big]. \quad (23)$$

Here, $\Psi'(z) = \left\{ \begin{array}{ll} \delta z^{\delta-1}, & \text{if } z \geq 0, \\ 0, & \text{if } z < 0 \end{array} \right\}$.

We also observe that the right-hand side in (23) can be represented as follows:

$$\begin{aligned} &\frac{1}{\varepsilon}\int_\Omega \left[\Psi'(\varphi^0_{\varepsilon,\tau} - l_{m+1}) - \Psi'(l_0 - \varphi^0_{\varepsilon,\tau})\right][\varphi - \varphi^0_{\varepsilon,\tau}]\, dx \\ &= \frac{2-\tau}{\varepsilon}\int_\Omega [\varphi - \varphi^0_{\varepsilon,\tau}] \\ &\times \left\{ \begin{array}{ll} (\varphi^0_{\varepsilon,\tau} - l_{m+1})^{1-\tau}, & \text{if } \varphi^0_{\varepsilon,\tau} - l_{m+1} > 0, \\ 0, & \text{otherwise} \end{array} \right\} dx \\ &- \frac{2-\tau}{\varepsilon}\int_\Omega [\varphi - \varphi^0_{\varepsilon,\tau}] \\ &\times \left\{ \begin{array}{ll} (l_0 - \varphi^0_{\varepsilon,\tau})^{1-\tau}, & \text{if } l_0 - \varphi^0_{\varepsilon,\tau} > 0, \\ 0, & \text{otherwise} \end{array} \right\} dx. \end{aligned} \quad (24)$$

Since $(c^0_{\varepsilon,\tau}, \varphi^0_{\varepsilon,\tau})$ is an optimal pair to the approximated minimization problem (8)–(12), it follows from representation (19)–(22) that

$$J_{\varepsilon,\tau}(c^0_{\varepsilon,\tau}, \varphi) - J_{\varepsilon,\tau}(c^0_{\varepsilon,\tau}, \varphi^0_{\varepsilon,\tau}) \geq 0 \quad \forall\, \varphi \in L^2(\Omega). \quad (25)$$

Taking into account that, for each $\varphi \in BV(\Omega)$,

$$\begin{aligned} &\Lambda_{\varepsilon,\tau}(\varphi) - \Lambda_{\varepsilon,\tau}\left(\varphi^0_{\varepsilon,\tau}\right) \\ &= \int_\Omega \left(L(\varphi) - L(\varphi^0_{\varepsilon,\tau})\right)|M^f_\varepsilon D\varphi^0_{\varepsilon,\tau}| \\ &+ \int_\Omega L(\varphi)|M^f_\varepsilon D\varphi| - \int_\Omega L(\varphi)|M^f_\varepsilon D\varphi^0_{\varepsilon,\tau}| \end{aligned} \quad (26)$$

with

$$L(\varphi) = \left(\varepsilon + \alpha \sum_{j=1}^m \delta_\varepsilon(\varphi - l_j + \tau)\right), \quad (27)$$

and setting

$$\begin{aligned} V_1\left(\varphi^0_{\varepsilon,\tau}\right) &= -\left(f - c^0_{\varepsilon,\tau,0}\right)\log\left(\frac{f}{c^0_{\varepsilon,\tau,0}}\right) \\ &\times \delta_\varepsilon(l_1 - \varphi^0_{\varepsilon,\tau} - \tau) \\ &+ \sum_{j=1}^{m-1}\left(f - c^0_{\varepsilon,\tau,j}\right)\log\left(\frac{f}{c^0_{\varepsilon,\tau,j}}\right) \\ &\times \delta_\varepsilon(\varphi^0_{\varepsilon,\tau} - l_j - \tau) H_\varepsilon(-\varphi^0_{\varepsilon,\tau} + l_{j+1} + \tau) \\ &- \sum_{j=1}^{m-1}\left(f - c^0_{\varepsilon,\tau,j}\right)\log\left(\frac{f}{c^0_{\varepsilon,\tau,j}}\right) \\ &\times \delta_\varepsilon(-\varphi^0_{\varepsilon,\tau} + l_{j+1} + \tau) H_\varepsilon(\varphi^0_{\varepsilon,\tau} - l_j - \tau) \\ &+ \left(f - c^0_{\varepsilon,\tau,m}\right)\log\left(\frac{f}{c^0_{\varepsilon,\tau,m}}\right)\delta_\varepsilon(\varphi^0_{\varepsilon,\tau} - l_m - \tau) \\ &+ \Big[\left\{ \begin{array}{l} (\varphi^0_{\varepsilon,\tau} - l_{m+1})^{1-\tau}, \quad \text{if } \varphi^0_{\varepsilon,\tau} - l_{m+1} > 0, \\ 0, \text{ otherwise,} \end{array} \right\} \\ &- \left\{ \begin{array}{l} (l_0 - \varphi^0_{\varepsilon,\tau})^{1-\tau}, \text{if } l_0 - \varphi^0_{\varepsilon,\tau} > 0, \\ 0, \text{ otherwise,} \end{array} \right\}\Big]\frac{2-\tau}{\varepsilon}, \end{aligned} \quad (28)$$

$$\mathcal{J}(w,\varphi) = \left\{ \begin{array}{ll} \displaystyle\int_\Omega L(w)\,|M^f_\varepsilon D\varphi| & \text{if } \varphi \in BV(\Omega), \\ +\infty & \text{if } \varphi \in L^2(\Omega) \setminus BV(\Omega), \end{array} \right. \quad (29)$$

$$V_2\left(\varphi^0_{\varepsilon,\tau}\right) = \alpha \sum_{j=1}^m \delta'_\varepsilon(\varphi^0_{\varepsilon,\tau} - l_j + \tau), \quad (30)$$

we see that inequality (25) leads to the relation

$$\begin{aligned} &\int_\Omega V_1\left(\varphi^0_{\varepsilon,\tau}\right)\varphi\, dx + \int_\Omega V_2\left(\varphi^0_{\varepsilon,\tau}\right)\varphi\,|M^f_\varepsilon D\varphi^0_{\varepsilon,\tau}| \\ &+ \left[\mathcal{J}(w,\varphi) - \mathcal{J}(w,\varphi^0_{\varepsilon,\tau})\right]\Big|_{w=\varphi} \geq o(1)h, \\ &\forall\, \varphi \in L^2(\Omega), \end{aligned} \quad (31)$$

where $h = \varphi - \varphi^0_{\varepsilon,\tau}$, and $o(1) \to 0$ as $\|h\|_{L^2(\Omega)} \to 0$.

Hence,

$$-V_1\left(\varphi^0_{\varepsilon,\tau}\right) \in \left[\partial\left(\int_\Omega V_2\left(\varphi^0_{\varepsilon,\tau}\right)\varphi\,|M^f_\varepsilon D\varphi^0_{\varepsilon,\tau}| + \mathcal{J}(w,\varphi)\right)\right]\Big|_{w=\varphi^0_{\varepsilon,\tau}}.$$

Since

$$\begin{aligned} &\partial\left(\int_\Omega V_2\left(\varphi^0_{\varepsilon,\tau}\right)\varphi\,|M^f_\varepsilon D\varphi^0_{\varepsilon,\tau}| + \mathcal{J}(w,\varphi)\right) \\ &= \partial\left(\int_\Omega V_2\left(\varphi^0_{\varepsilon,\tau}\right)\varphi\,|M^f_\varepsilon D\varphi^0_{\varepsilon,\tau}|\right) + \partial\mathcal{J}(w,\varphi) \end{aligned}$$

by the Moreau–Rockafellar Theorem, it follows that the Euler–Lagrange equation for $\varphi^0_{\varepsilon,\tau}$ takes

the form

$$\partial\left(\int_\Omega V_2\left(\varphi^0_{\varepsilon,\tau}\right)\varphi\,|M^f_\varepsilon D\varphi^0_{\varepsilon,\tau}|\right)+ \partial\mathcal{J}(w,\varphi)|_{w=\varphi^0_{\varepsilon,\tau}}+V_1\left(\varphi^0_{\varepsilon,\tau}\right)\ni 0. \quad (32)$$

Following Anzellotti,[32] for an open bounded set with Lipschitz boundary $\Omega\subset\mathbb{R}^2$, we denote

$$X_2(\Omega)=\left\{z\in L^\infty(\Omega;\mathbb{R}^2)\,:\,\mathrm{div}(z)\in L^2(\Omega)\right\} \quad (33)$$

to give a correct interpretation of the Anzelotti pairing (z,Du) with $u\in BV(\Omega)$. In this case, if $u\in BV(\Omega)$ and $z\in X_2(\Omega)$, then for every test function $\psi\in C^\infty_0(\Omega)$, we have

$$\langle(z,Du),\psi\rangle:=-\int_\Omega u\,\mathrm{div}(\psi z)\,dx= -\int_\Omega u\psi\,\mathrm{div}(z)\,dx-\int_\Omega u(z,\nabla\psi)\,dx. \quad (34)$$

Arguing as in,[?Proposition 4.1.]Vese it can be shown that $\xi\in\partial\mathcal{J}(w,\varphi)|_{w=\varphi^0_{\varepsilon,\tau}}$ if and only if there exists a vector field $\boldsymbol{z}\in X_2(\Omega)$ (see (33)) such that the following conditions hold:

$$\|\boldsymbol{z}\|_{L^\infty(\Omega;\mathbb{R}^2)}\le 1,$$
$$\left(\boldsymbol{z},M^f_\varepsilon D\varphi^0_{\varepsilon,\tau}\right)=\left|M^f_\varepsilon D\varphi^0_{\varepsilon,\tau}\right| \quad \text{as measures},$$
$$-\mathrm{div}\left(L(\varphi^0_{\varepsilon,\tau})M^f_\varepsilon\boldsymbol{z}\right)=\xi \quad \text{in } \Omega,$$
$$\left[L(\varphi^0_{\varepsilon,\tau})M^f_\varepsilon\boldsymbol{z},\nu_\Omega\right]=0 \quad \text{a.e. on } \partial\Omega.$$

Then taking into account the Anzelotti representation (34) and the fact that

$$-\mathrm{div}\left(L(\varphi^0_{\varepsilon,\tau})M^f_\varepsilon\boldsymbol{z}\right) =-V_2\left(\varphi^0_{\varepsilon,\tau}\right)\left(M^f_\varepsilon D\varphi^0_{\varepsilon,\tau},\boldsymbol{z}\right) -L(\varphi^0_{\varepsilon,\tau})\,\mathrm{div}\left(M^f_\varepsilon\boldsymbol{z}\right) =-V_2\left(\varphi^0_{\varepsilon,\tau}\right)\left|M^f_\varepsilon D\varphi^0_{\varepsilon,\tau}\right|-L(\varphi^0_{\varepsilon,\tau})\,\mathrm{div}\left(M^f_\varepsilon\boldsymbol{z}\right)$$

we can finally rewrite (32) as follows

$$-L(\varphi^0_{\varepsilon,\tau})\,\mathrm{div}\left(M^f_\varepsilon\boldsymbol{z}\right)+V_1\left(\varphi^0_{\varepsilon,\tau}\right)\ni 0, \quad (35)$$
$$\left[L(\varphi^0_{\varepsilon,\tau})M^f_\varepsilon\boldsymbol{z},\nu_\Omega\right]=0 \quad \text{a.e. on } \partial\Omega, \quad (36)$$
$$\left(\boldsymbol{z},M^f_\varepsilon D\varphi^0_{\varepsilon,\tau}\right)=\left|M^f_\varepsilon D\varphi^0_{\varepsilon,\tau}\right|, \quad (37)$$
$$\|\boldsymbol{z}\|_{L^\infty(\Omega;\mathbb{R}^2)}\le 1. \quad (38)$$

If in addition $\varphi^0_{\varepsilon,\tau}$ is differentiable in the weak sense, then the Euler–Lagrange system (35)–(38) assumes the form of the following boundary value problem:

$$-L(\varphi^0_{\varepsilon,\tau})\,\mathrm{div}\left(M^f_\varepsilon\frac{M^f_\varepsilon\nabla\varphi^0_{\varepsilon,\tau}}{|M^f_\varepsilon\nabla\varphi^0_{\varepsilon,\tau}|}\right)+V_1\left(\varphi^0_{\varepsilon,\tau}\right)=0 \quad \text{in } \mathcal{D}'(\Omega), \quad (39)$$

$$\left(M^f_\varepsilon\frac{M^f_\varepsilon\nabla\varphi^0_{\varepsilon,\tau}}{|M^f_\varepsilon\nabla\varphi^0_{\varepsilon,\tau}|},\nu_\Omega\right)=0 \quad \text{a.e. on } \partial\Omega. \quad (40)$$

4. Numerical approximation of the optimality conditions

In this section, we briefly describe the numerical scheme and a procedure to solve the Euler–Lagrange system (39)–(40) numerically. Since for implementations, it is reasonable to define the solution of the problem (39)–(40) using a "gradient descent"strategy, denoted by S a given circle and by $d(x,S)$ the Euclidean distance of the point $x\in\Omega$ from the circle S, we suggest starting with the initial level function $\varphi_0\in C(\Omega)$ that can be defined as follows (see also the other variants in[19])

$$\varphi_0(x)=\begin{cases}+d(x,S), & x\in\text{inside}\,S,\\ 0, & x\in S,\\ -d(x,S), & x\in\text{outside}\,S.\end{cases} \quad (41)$$

Next, for numerical purposes, we calculate $u_{\varepsilon,\tau}$, the continuous approximation of the BV solution $\varphi^0_{\varepsilon,\tau}$, with $\varepsilon>0$ and $\tau>0$ small enough, as a solution of the problem

$$\frac{\partial\varphi}{\partial t}=L(\varphi)\,\mathrm{div}\left(M^f_\varepsilon\frac{M^f_\varepsilon\nabla\varphi}{|M^f_\varepsilon\nabla\varphi|}\right)-V_1(\varphi) \quad \text{in } (0,\infty)\times\Omega, \quad (42)$$

$$\left(M^f_\varepsilon\frac{M^f_\varepsilon\nabla\varphi}{|M^f_\varepsilon\nabla\varphi|},\nu_\Omega\right)=0 \text{ on } (0,\infty)\times\partial\Omega, \quad (43)$$

$$\varphi(0,\cdot)=\varphi_0(\cdot) \text{ in } \Omega. \quad (44)$$

The second point that we realize in this algorithm is to consider the adaptive version of the model (42)–(44). Following[19] and,[34] we substitute the multipliers $\delta_\varepsilon(-\varphi^0_{\varepsilon,\tau}+l_{j+1}+\tau)$ in the external force $V_1(\varphi)$ with 1. It has been recently shown in[34] that, in this way, the external force without $\delta_\varepsilon(-\varphi^0_{\varepsilon,\tau}+l_{j+1}+\tau)$ can take action on φ everywhere in Ω (not simply on the prescribed level sets of φ), and so can keep φ moving more quickly towards the desired segment edges. As a result, the adaptive version of the external force $V_1(\varphi)$ takes the form

$$\widehat{V}_1(\varphi)=-\left(f-c^0_{\varepsilon,\tau,0}\right)\log\left(\frac{f}{c^0_{\varepsilon,\tau,0}}\right)$$

$$+\left(f-c^0_{\varepsilon,\tau,m}\right)\log\left(\frac{f}{c^0_{\varepsilon,\tau,m}}\right)$$
$$+\sum_{j=1}^{m-1}\left(f-c^0_{\varepsilon,\tau,j}\right)\log\left(\frac{f}{c^0_{\varepsilon,\tau,j}}\right)$$
$$[H_\varepsilon(-\varphi+l_{j+1}+\tau)-H_\varepsilon(\varphi-l_j-\tau)]$$
$$+\frac{2-\tau}{\varepsilon}\left\{\begin{array}{l}(\varphi-l_{m+1})^{1-\tau},\quad \text{if } \varphi-l_{m+1}>0,\\ 0,\ \text{otherwise},\end{array}\right\}$$
$$-\frac{2-\tau}{\varepsilon}\left\{\begin{array}{ll}(l_0-\varphi)^{1-\tau}, & \text{if } l_0-\varphi>0,\\ 0, & \text{otherwise.}\end{array}\right\} \quad (45)$$

We also need to specify the boundary condition on $\partial\Omega$ associated with (43). To obtain a well-posed problem, we change the natural boundary condition (43) just slightly, namely

$$\left(M^f_\varepsilon\frac{M^f_\varepsilon\nabla\varphi}{\sqrt{\varepsilon^2+|M^f_\varepsilon\nabla\varphi|^2}},\nu_\Omega\right)=0 \quad \text{a.e. on } \partial\Omega.$$

Because the denominator $\sqrt{\varepsilon+|M^f_\varepsilon\nabla\varphi|^2}$ is strictly positive, the matrix function $M^f_\varepsilon(x)$ for each $x\in\Omega$ is symmetric, and the discrete gradients are bounded in the norm, we can pass to the following boundary condition instead of (43)

$$\left(M^f_\varepsilon\nabla\varphi, M^f_\varepsilon\nu_\Omega\right)=0 \quad \text{on } \partial\Omega, \qquad (46)$$

where ν_Ω is a unit normal to $\partial\Omega$. However, in view of the assumption (6), this condition can be rewritten as follows:

$$\frac{\partial\varphi}{\partial\nu_\Omega}=0 \quad \text{on } \partial\Omega.$$

Consequently, we obtain the subsequent problem for numerical simulation

$$\frac{\partial\varphi}{\partial t}=L(\varphi)\,\mathrm{div}\left(\frac{\left(M^f_\varepsilon\right)^2\nabla\varphi}{\sqrt{\varepsilon^2+|M^f_\varepsilon\nabla\varphi|^2}}\right)-\widehat{V}_1(\varphi)$$
$$\text{in } (0,\infty)\times\Omega, \qquad (47)$$
$$\frac{\partial\varphi}{\partial\nu_\Omega}=0 \quad \text{on } (0,\infty)\times\partial\Omega, \qquad (48)$$
$$\varphi(0,\cdot)=\varphi_0(\cdot) \quad \text{in } \Omega, \qquad (49)$$

where the functions $L(\varphi)$ and $\widehat{V}_1(\varphi)$ are defined by (27) and (45), respectively.

Quasi-linear partial differential equations can be solved in a variety of ways (for a list of methods, check the references[35,36]). Finite differences techniques and an explicit scheme of the forward Euler method are maybe the best choices because we are working with pixels in image processing. Let Δt be a time step size. Then setting

$$t=n\Delta t,\ n=0,1,2,\ldots,$$
$$x=i\ (1\le i\le N_x),\quad y=j\ (1\le j\le N_y),$$

where (x,y) stands for image pixel and $N_x\times N_y$ is the original image size at the grid G_H, we define the following discrete notations

$$\Delta^x_\pm\varphi^n_{ij}=\pm\left(\varphi^n_{i\pm1,j}-\varphi^n_{ij}\right),$$
$$\Delta^y_\pm\varphi^n_{ij}=\pm\left(\varphi^n_{i,j\pm1}-\varphi^n_{ij}\right),$$
$$m(a,b)=\mathrm{minmod}\,(a,b)=$$
$$\min\left(|a|,|b|\right)\frac{\mathrm{sgn}\,a+\mathrm{sgn}\,b}{2},$$

where $\varphi^n_{i,j}$ denotes the approximation of $\varphi_{k+1}(n\Delta t,i,j)$. Then, the numerical approximation of the principle components of the boundary value problem (47)–(49) takes the form

$$\left(\frac{\partial\varphi}{\partial t}\right)^n_{i,j}\approx\frac{\varphi^{n+1}_{i,j}-\varphi^n_{i,j}}{\Delta t},$$
$$\left(\mathrm{div}\left(\frac{\left(M^f_\varepsilon\right)^2\nabla\varphi}{\sqrt{\varepsilon^2+|M^f_\varepsilon\nabla\varphi|^2}}\right)\right)^n_{i,j}\approx$$
$$\Delta^x_-\left(X^n_{i,j}\right)+\Delta^y_-\left(Y^n_{i,j}\right),$$
$$X^n_{i,j}=aP^n_{i,j}+bQ^n_{i,j},\quad Y^n_{i,j}=bP^n_{i,j}+cQ^n_{i,j},$$
$$\left(\begin{array}{cc}a & b\\ b & c\end{array}\right)=\left(M^f_\varepsilon\right)^2,$$
$$P^n_{i,j}=\frac{\Delta^x_+\varphi^n_{i,j}}{\sqrt{\varepsilon^2+\left(\Delta^x_+\varphi^n_{i,j}\right)^2+\left(m\left(\Delta^y_+\varphi^n_{i,j},\Delta^y_-\varphi^n_{i,j}\right)\right)^2}},$$
$$Q^n_{i,j}=\frac{\Delta^y_+\varphi^n_{i,j}}{\sqrt{\varepsilon^2+\left(\Delta^y_+\varphi^n_{i,j}\right)^2+\left(m\left(\Delta^x_+\varphi^n_{i,j},\Delta^x_-\varphi^n_{i,j}\right)\right)^2}}.$$

As a result, utilizing the formulas given above, we arrive at the following numerical scheme associated with the initial boundary problem (47)–(49):

$$\varphi^{n+1}_{i,j}=\varphi^n_{i,j}+L(\varphi^n_{i,j})$$
$$\times\left(\Delta^x_-\left[X^n_{i,j}\right]+\Delta^y_-\left[Y^n_{i,j}\right]\right)\Delta t-\widehat{V}_1(\varphi^n_{l,j})\Delta t$$
$$\forall i=1,\ldots,N_x,\quad \forall j=1,\ldots,N_y,$$
$$\forall n=0,1,\ldots \qquad (50)$$

with the initial conditions

$$\varphi^0_{i,j}=(\varphi_0)_{i,j},$$
$$\forall i=1,\ldots,N_x,\quad \forall j=1,\ldots,N_y, \qquad (51)$$

and boundary conditions

$$\varphi^n_{0,j}=\varphi^n_{1,j},\quad \varphi^n_{N_x,j}=\varphi^n_{N_x-1,j},$$
$$v^n_{l,0}=v^n_{l,1},\quad \varphi^n_{l,N_y}=\varphi^n_{l,N_y-1}, \qquad (52)$$
$$\forall l=1,\ldots,N_x,\quad \forall j=1,\ldots,N_y.$$

Since the set-level function $\varphi(x)$ should be subjected by the constraints (see (4))

$$l_0 \le \varphi(x) \le l_{m+1} \text{ a.e. in } \Omega,$$

in practice this constraint can be incorporated by renormalizing $\varphi^n_{i,j}$ (when $\varphi^n_{i,j} < l_0$ or $\varphi^n_{i,j} > l_{m+1}$) after each time step. It means that we can omit the last two terms in the external force $\widehat{V}_1(\varphi)$ that emerge as the penalizing ones. As a result, we can modify the iteration procedure (50) as follows:

$$\begin{aligned}\varphi^{n+1}_{i,j} &= \varphi^n_{i,j} + L(\varphi^n_{i,j})\left(\Delta^x_-\left[X^n_{i,j}\right] + \Delta^y_-\left[Y^n_{i,j}\right]\right)\Delta t \\ &+ \left(f - c^0_{\varepsilon,\tau,0}\right)\log\left(\frac{f}{c^0_{\varepsilon,\tau,0}}\right) \\ &- \left(f - c^0_{\varepsilon,\tau,m}\right)\log\left(\frac{f}{c^0_{\varepsilon,\tau,m}}\right) \\ &- \sum_{j=1}^{m-1}\left(f - c^0_{\varepsilon,\tau,j}\right)\log\left(\frac{f}{c^0_{\varepsilon,\tau,j}}\right) \\ &\times \left[H_\varepsilon(-\varphi^n_{i,j} + l_{j+1} + \tau) - H_\varepsilon(\varphi^n_{i,j} - l_j - \tau)\right], \end{aligned} \tag{53}$$

$$\varphi^{n+1}_{i,j} = l_0 \quad \text{if} \quad \varphi^{n+1}_{i,j} < l_0, \tag{54}$$

$$\varphi^{n+1}_{i,j} = l_{m+1} \quad \text{if} \quad \varphi^{n+1}_{i,j} > l_{m+1}, \tag{55}$$

$$\forall i = 1,\dots,N_x, \quad \forall j = 1,\dots,N_y, \quad \forall n = 0,1,\dots$$

Taking into account the following estimates:

$$\left(M^f_\varepsilon\right)^2 \le I \quad \text{in the sense of quadratic forms,}$$

$$|P^n_{i,j}| \le \frac{1}{\varepsilon}|\Delta^x_+\varphi^n_{i,j}|, \quad |Q^n_{i,j}| \le \frac{1}{\varepsilon}|\Delta^y_+\varphi^n_{i,j}|,$$

$$L(\varphi^n_{i,j}) \le \varepsilon + \alpha\frac{m}{\varepsilon}$$

and arguing as in[?Chapter 28]Salgado, we can deduce the following stability conditions for the proposed approximation scheme

$$\Delta t\left(1 + \alpha\frac{m}{\varepsilon^2}\right) < \frac{1}{2}. \tag{56}$$

Therefore, the stability of the numerical scheme (51),(52),(53)–(55) depends critically on the parameter $\alpha > 0$ being chosen correctly. As for the stopping condition, it can be formalized as follows:

$$\max_{1\le i\le N_x}\max_{1\le j\le N_y}\left|\varphi^{n+1}_{i,j} - \varphi^n_{l,j}\right| \le \varepsilon.$$

Our next intention in this section is to discuss the algorithm for restoration and visualization of the level sets

$$S_j := \{x \in \Omega : \varphi(x) = l_j\}, \quad j = 1,2,\dots,m.$$

Definition 1. *Let $f : \Omega \to \mathbb{R}$ be a gray-scale image satisfying conditions (2). Let $\varphi^0_{\varepsilon,\tau} \in BV(\Omega)$ be a solution of the minimization problem (8)–(12) with $\varepsilon > 0$ and $\tau > 0$ small enough. Let $\left(\varphi^0_{\varepsilon,\tau}\right)_\rho \in C^\infty(\overline{\Omega})$ be the smoothed version as the convolution of the 2-D Gaussian kernel G_ρ and $\varphi^0_{\varepsilon,\tau}$. We say that the following decomposition*

$$\Omega = \Omega_0 \cup \Omega_1 \cup \dots \cup \Omega_m \cup \Omega_*$$

is quasi-optimal for the approximation of f by piecewise constant function $f_* : \Omega \to \mathbb{R}$ if

- *the restrictions $f_*|_{\Omega_j}$ are defined as*

$$f_*|_{\Omega_j} = c^0_{\varepsilon,\tau,j}, \quad j = 0,\dots,m,$$

where the constants $c^0_{\varepsilon,\tau,j}$ are given by (16);

- *the subdomains (or segments) $\{\Omega_j\}_{j=0}^m$ are related to the function $\varphi^0_{i,j}$ as follows*

$$\Omega_0 = \left\{x \in \Omega : \left(\varphi^0_{\varepsilon,\tau}\right)_\rho(x) < l_1\right\}, \tag{57}$$

$$\Omega_j = \left\{x \in \Omega : l_j < \left(\varphi^0_{\varepsilon,\tau}\right)_\rho(x) < l_{j+1}\right\}, \tag{58}$$

$$j = 1,\dots,m-1,$$

$$\Omega_m = \left\{x \in \Omega : \left(\varphi^0_{\varepsilon,\tau}\right)_\rho(x) > l_m\right\}; \tag{59}$$

- *Ω_* stands for the boundaries between different Ω_j, that is,*

$$\Omega_* = \bigcup_{j=1}^m \left\{x \in \Omega : \left(\varphi^0_{\varepsilon,\tau}\right)_\rho(x) = l_j\right\}.$$

As immediately follows from this definition, each segment Ω_j of the given f-decomposition can be associated with the corresponding coefficient of variation CV_j, $j = 0,\dots,m$. This coefficient is the measure that quantifies the degree of variability in the set of data by calculating the ratio of the standard deviation of $f(x)$ within Ω_j to its mean $f_*|_{\Omega_j}$, that is,

$$CV_j = \frac{\sqrt{\int_{\Omega_j}\left(f(x) - f_*|_{\Omega_j}(x)\right)^2 dx}}{f_*|_{\Omega_j}}$$

for all $j = 0,\dots,m$.

Thus, by this definition, the boundaries $\partial\Omega_j$ of the segments Ω_j can be defined as the corresponding level sets S_j. To identify these sets, we make use of the so-called marching squares method.[38,39] The main steps of this approach can be described as follows:

(1) Given an index $j \in \{1,\dots,m\}$ and a smoothed version $\left(\varphi^0_{\varepsilon,\tau}\right)_\rho \in C^\infty(\overline{\Omega})$ of the level set function $\varphi^0_{\varepsilon,\tau} \in BV(\Omega)$, create a binary image $\mathfrak{B}_j$ following the rule

$$\mathfrak{B}_j(x) = \begin{cases} 1, & \text{if } \left(\varphi^0_{\varepsilon,\tau}\right)_\rho(x) \ge l_j, \\ 0, & \text{if } \left(\varphi^0_{\varepsilon,\tau}\right)_\rho(x) < l_j, \end{cases} \quad \forall x \in \Omega.$$

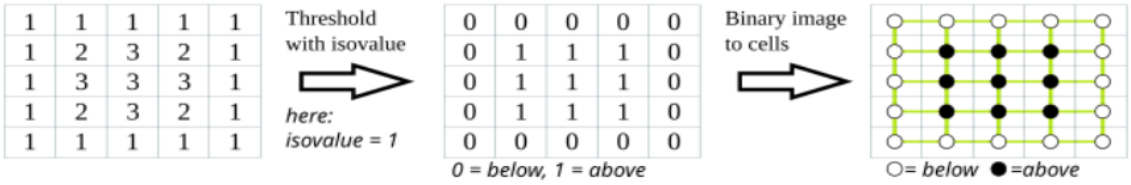

Figure 1. Binary image $\mathfrak{B}_j$ with $l_j = 1$

Then every 2×2 block of pixels in the binary image forms a contouring cell, so the whole image is represented by a grid of such cells (see Fig.1). In fact, just for illustration, this picture reflects the main actions that we have to do in order to find out a correct location of the level set $\left(\varphi^0_{\varepsilon,\tau}\right)_\rho(x) = 1.5$.

(2) Follow these steps for every cell in the contouring grid:

(a) To create a binary index, combine the 4 bits at the cell's corners: Using the bitwise OR and left-shift, go clockwise around the cell from the most significant bit at the top left to the least significant bit at the bottom left, adding the bit to the index. As indicated in the table below, the resulting 4-bit index has 16 potential values in the range $0 - 15$.

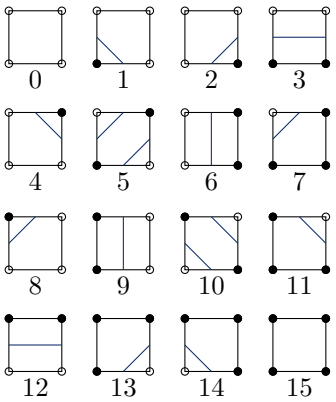

(b) Utilize the cell index to access a prebuilt lookup table with 16 entries that list the edges required to represent the cell.

(c) To determine the precise location of the contour line along the cell's edges, use linear interpolation between the initial field data values. (see Fig. 2).

5. Numerical Results

In this section, we dwell on two possible ways for the implementation of the proposed approach to domain decomposition. We call these ways just direct and adaptive segmentation procedures. The key point of the direct segmentation is the fact that the number $m+1$ of segments that must correspond to the homogeneity zones of a given function $f : \Omega \to \mathbb{R}$, should be prescribed a priori, provided the degree of variability of the original distribution $f : \Omega \to \mathbb{R}$ over Ω satisfies the condition

$$CV\left(f\big|_\Omega\right) = \frac{\sigma\left(f\big|_\Omega\right)}{\text{mean}\left(f\big|_\Omega\right)} \cdot 100\% > \delta_{\min},$$

where $\delta_{\min} > 0$ is a given threshold. Typically, a distribution f is considered homogeneous, especially in the agricultural application, if $CV(f\big|_\Omega) \leq 15\%$.

To illustrate the efficiency of the proposed model and the scheme of direct segmentation, we provided numerical experiences with images that the Sentinel-2 satellite has delivered. we used a 10 m/pixel image over the Dnipro region of Ukraine as input data (see the left panel in Figure 3).

With medium-sized fields of different shapes, this area exemplifies a typical agricultural landscape. The observed data suffer from noise and blurring, as can be seen from the image in Fig. 3 (also refer to the related histogram in Fig. 4).

Using the variational approach recently proposed in[40] (see also[7,8]), we implemented the deblurring and denoizing procedure as the first stage (see the right panel in Fig. 3). The smoothed picture histogram has a marked compactly localized spectrum, as shown in Figure 4. This spectrum could be regarded as a "good option"for its piecewise constant approximation.

Numerical simulations of f-decomposition following the scheme of the direct segmentation have been performed considering three different variants setting $f(x) = u_i(x)$, in Ω, where u_i with $i = 1, 2, 3$ stands for the intensity of the satellite image at the left panel of Figure 1 in red, blue, and green spectral channels, respectively. To define a segmentation in each of these channels, we applied the iteration procedure (51), (52), (53)–(55) to the corresponding function $f = u_i$ with

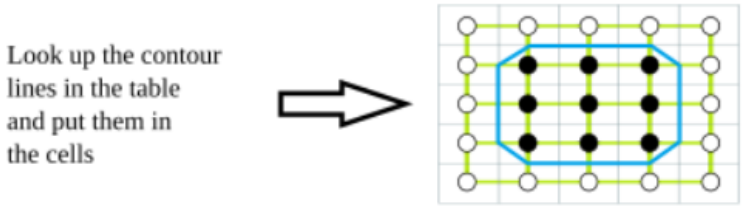

Figure 2. Variant of the contour lines in the cell

Figure 3. On the left: The original satellite photo. On the right: The photo after denoising

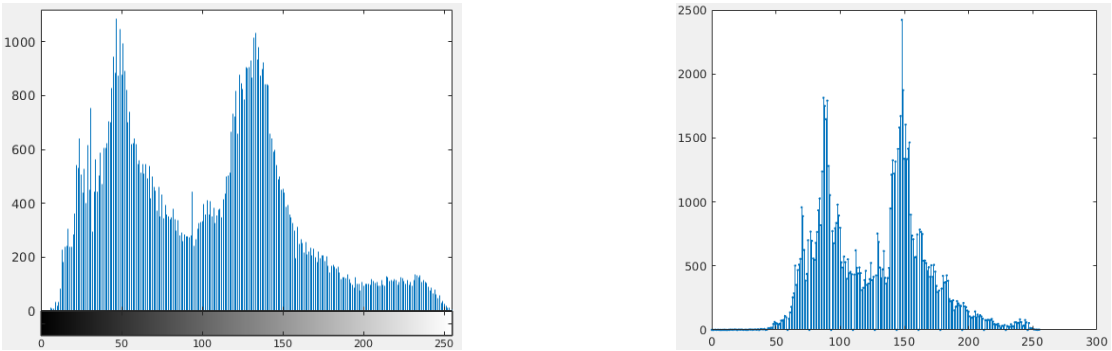

Figure 4. On the left: Histogram of the original image. On the right: Histogram of the smoothed data

the following setting

$$m = 3, \quad l_0 = -20000, \quad l_1 = -18000,$$
$$l_2 = -2000, \quad l_3 = 10000, \quad l_4 = 20000,$$
$$\sigma = 3, \quad \tau = 0.1, \quad \eta = 1 - \varepsilon,$$
$$\varepsilon = 0.01, \quad \Delta t = 0.05,$$

and $\varphi_0 \in C(\Omega)$ of (41), the initial level set function, was taken with S circle having radius 20 and center in the central point of Ω, and $d(x, S)$ the Euclidean distance between the point $x \in \Omega$ and S.

The parameter α is defined by the rule (56). Results of segmentation that have been obtained in this way, are depicted in Fig. 5–6. In fact, the given f-decomposition can be drilled down for each channel by iterative setting $\Omega = \Omega_i$, $i = 1, 2$, and so on. Regarding the procedure's stop-condition, it can be taken as follows:

$$\text{either} \quad \mathcal{L}^2(\Omega_i) < \delta_1 \quad \text{or} \quad CV\left(f\big|_{\Omega_i}\right) < \delta_2$$

for given $\delta_1, \delta_2 > 0$.

However, it should be emphasized that the main drawback of the direct approach to the segmentation procedure is the fact that the final result (the shape of the obtained segments, their area, and the corresponding coefficient of variation) crucially depends on the number of segments $m+1$ that we prescribe as an input characteristic. To circumvent this restriction, we make use of the adaptive approach. In this context, we do not fix a priori the number of segments, but instead, we decompose the interval $[l_0, l_{m+1}]$ into a uniform grid

$$l_0 < l_1 < l_2 < \cdots < l_{M-1} < l_M < l_{m+1}$$

with $l_j = l_0 + j\Delta l$, where the integer $M > 0$ satisfies the condition

$$\frac{|\Omega|}{M+1} \approx S^*.$$

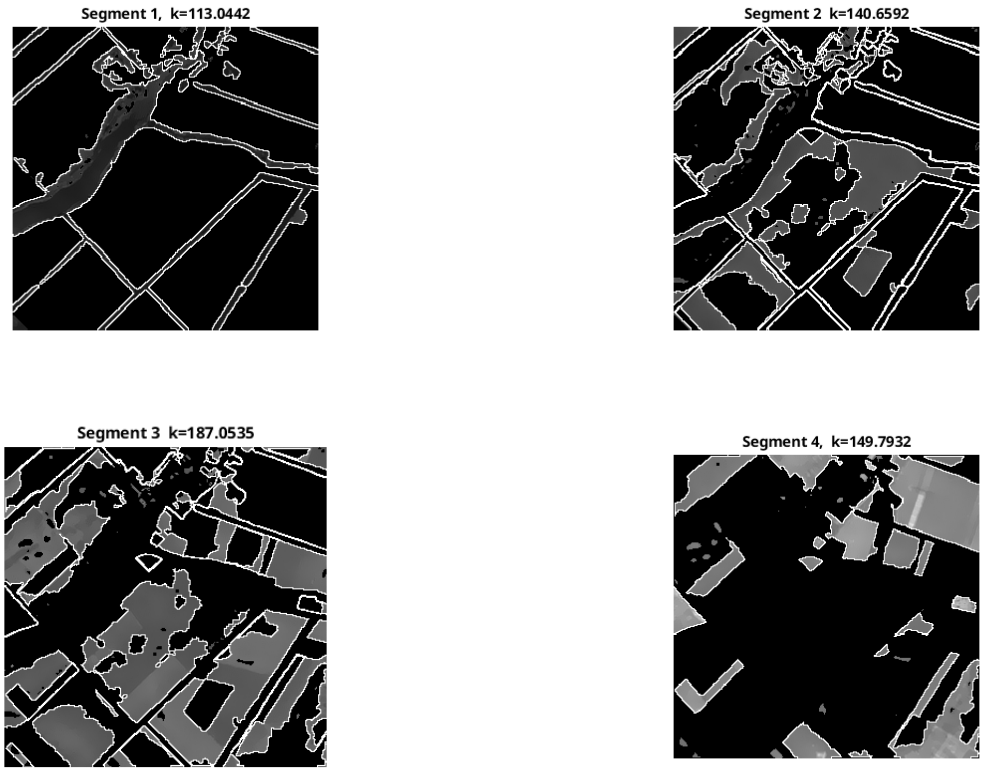

Figure 5. f-decomposition with $f(x) = u_{red}(x)$

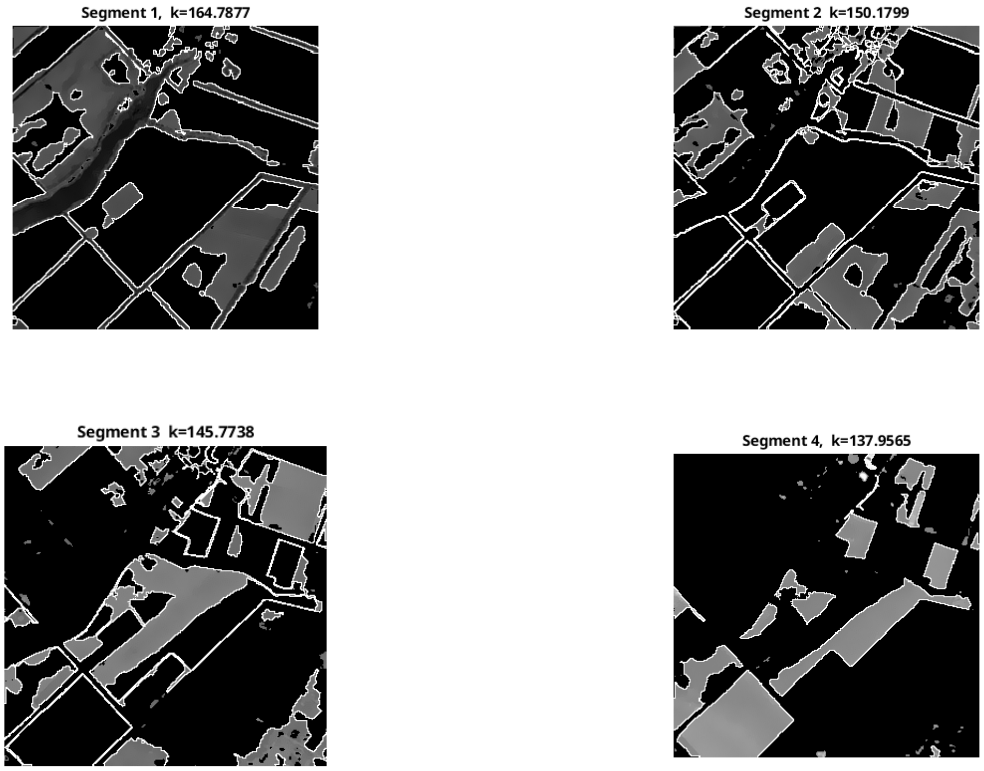

Figure 6. f-decomposition with $f(x) = u_{green}(x)$

Here, S^* stands for the area of a standard field in a given region.

After that we define the function $\varphi^0_{\varepsilon,\tau}$ as a solution of the problem (51), (52), (53)–(55) with the given collection $\{l_j\}_{j=1}^M$. Let $\{S_j\}_{j=0}^M$ be a set of the corresponding segments that we identify by the rules (57)–(59). Then we define the true segments as follows:

```
k=1;
True_Segment(k):=S_0;
for j=1:M
  if area(S_1)<0.10 S*
     combine{True_Segment(k),S_j};
  else
 k=k+1;
 True_Segment(k):=S_j;
end
Number_of_true_Segments:=k;
```

Here, the multiplier 0.10 emerges as a part of the field that can be neglected as a zone of inhomogeneity.

6. Conclusion

The generalized active contour model, proposed in,[1] to extract agricultural crop fields with a high degree of inhomogeneity from satellite data has been implemented. Setting an optimization problem, it was possible to achieve a disjunctive decomposition of a given field into a finite number of non-empty subsets, each of which could be associated with a unique value of an agricultural index. The Euler–Lagrange equation with the appropriate initial and boundary conditions has been used to express the corresponding optimality system under certain assumptions. A method for the numerical solution of the Euler–Lagrange system has been provided along with a numerical scheme. Using a direct approach to the segmentation technique and the new adaptive one, numerical simulations utilizing real-life satellite images have been conducted to show the accuracy and effectiveness of the proposed model.

Acknowledgments

None.

Funding

None.

Conflict of interest

The authors declare no conflict of interest.

Author contributions

Conceptualization: All authors
Formal analysis: All authors
Investigation: All authors
Methodology: All authors
Writing-original draft: All authors
Writing-review & editing: All authors

Availability of data

Not applicable.

References

1. D'Apice C., Kogut PI, Manzo R. On generalized active contour model in the anisotropic BV space and its application to satellite remote sensing of agricultural territory. *Netw Heterogen Media.* 2025;20(1): 113-142.
2. Mulla DJ. Twenty five years of remote sensing in precision agriculture: key advances and remaining knowledge gaps. *Biosyst Eng.* 2013; 114(4):358-371.
3. Xue J, Su B. Significant remote sensing vegetation indices: a review of developments and applications. *Hindawi J Sens.* 2017;2017:1-17. (Article ID 1353691)
4. Hnatushenko VV, Kogut PI, Uvarov M. Variational approach for rigid co-registration of optical/SAR satellite images in agricultural areas. *J Comput Appl Math.* 2022;400:15. Id 113742.
5. Khanenko P, Kogut PI, Uvarov M. On variational problem with nonstandard growth conditions for the restoration of clouds corrupted satellite images. In: *CEUR Workshop Proceedings, the 2nd International Workshop on Computational and Information Technologies for Risk-Informed Systems, CITRisk-2021*, September 16-17, 2021, Kherson, Ukraine, Vol. 3101; 2021: 6-25.
6. Ivanchuk N, Kogut PI, Martyniuk P. On generation of daily cloud free images at a high resolution level. In: M. Zgurovsky, N. Pankratova, eds. *System Analysis and Artificial Intelligence. Studies in Computational Intelligence*, Vol 1107. Cham: Springer; 2023: 203-232.
7. D'Apice C, Kogut PI, Manzo R. A two-level variational algorithm in the Sobolev-Orlicz space to predict daily surface reflectance at LANDSAT high spatial resolution and MODIS temporal frequency. *J Comput Appl Math.* 2023;434:115339.
8. D'Apice C, Kogut PI, Manzo R, Uvarov M. Variational model with nonstandard growth conditions for the restoration of satellite optical images using synthetic aperture radar. *Eur J Appl Math.* 2023; 34(1):77-105.
9. Hnatushenko VV, Kogut PI, & Uvarov MV. On satellite image Segmentation via piecewise constant approximation of selective smoothed target mapping. *Appl Math Comput.* 2021;389:125615.

10. Kogut PI, Kupenko OP, Uvarov NV. On increasing of resolution of satellite images via their fusion with imagery at higher resolution. *J Optimiz DiffEquat Appl.* 2021;29(1):54-78.
11. Mumford D, Shah J. Optimal approximation by piecewise smooth functions and associated variational problems. *Commun Pure Appl Math.* 1989;42(5):577-685.
12. Alvarez L, Lions PL, Morel J-M. Image selective smoothing and edge detection by nonlinear diffusion. II. *SIAM J Numer Anal.* 1992;9(3):845-866.
13. Caselles V, Kimmel R, Sapiro G. Geodesic active contours. *Int J Comput Vis.* 1997;22(1):61-79.
14. Chan T, Vese L. Active contours without edges. *IEEE Trans Image Process.* 2001;10(2):266-277.
15. Alvarez L, Guichard F, Lions PL, Morel J-M. Axioms and fundamental equations of image processing. *Arch Ration Mech Anal.* 1993;123(3):199-257.
16. Catté F, Coll T, Lions PL, J-M. Image selective smoothing and edge detection by nonlinear diffusion. I. *SIAM J Numer Anal.* 1992;29(1):182-193.
17. Yang C, Weng G, Chen Y. Active contour model based on local Kullback-Leibler divergence for fast image segmentation. *Eng Appl Artif Intell.* 2023;123:106472.
18. Han B, Wun Y. Active contour model for inhomogenous image segmentation based on Jeffreys divergence. *Pattern Recognit.* 2020;107: 1075202.
19. Yuan Y., He C. Adaptive active contours without edges. *Math Comput Modell.* 2012;55:1705-1721.
20. Kass M, Witkin A, Terzopoulos D. Snakes: active contour models. *Int J Comput Vis.* 1988;1(4):321-331.
21. Dai L, Ding J, Yang J. Inhomogeneity-embedded active contour for natural image segmentation. *Pattern Recognit.* 2015;48(8):2513-2529.
22. Chen Y, Wu L, Wang G, Weng G, Chen H. An active contour model for image segmentation using morphology and nonlinear Poisson's equation. *Optik.* 2023;287: 170997.
23. Fang L, Liang X, Xu C, Wang Q. Image segmentation using a novel dual active contour model. *Multimedia Tools Appl.* 2024;83(2):3707-724.
24. Ge P, Chen Y, Wang G, Weng G. An active contour model based on Jeffreys divergence and clustering technology for image segmentation. *J Vis Commun Image Represent.* 2024;99:104069.
25. Kon NA, Jumaat AK, Suhaizi MDA. Active contour models for boundary extraction with application to medical images with noise. *J Adv Res ApplSciEng Technol.* 2024;33(2):300-312.
26. Mazlin MS, Jumaat AK, Embong R. Partitioning intensity inhomogeneity colour images via Saliency-based active contour. *Int J Elect Comput Eng.* 2024;14(1):337-346.
27. Suryana ME, Rizki M, Irzal M, Aryani R. Solving wound perimeter detection with active contour model enhanced with interpolation. *AIP Conf Proc.* 2024;2982(1):060005.
28. Zhang M, Meng D, Pei Y, Wen J. Research on image segmentation method based on improved Snake model. *Multimedia Tools Appl.* 2024;83(5):13977-13994.
29. Ivanchuk N, Kogut PI, Kupenko O. Generalized active contour model in an anisotropic variable exponent Sobolev space. *J Optimiz Diff Equat Appl.* 2024;32(1):1-32.
30. Kogut PI, Kohut Ya, Parfinovych N. Solvability issues for some noncoercive and nonmonotone parabolic
equations arising in the image denoising problems. *J Optimiz Differ Equat Appl.* 2022;30(2):19-48.
31. Kogut PI, Kohut Y, Manzo R. Fictitious controls and approximation of anÂ optimal control problem for Perona-Malik equation. J Optimiz *Differ Equat Appl.* 2022;30(1):42-70.
32. Anzellotti G. Pairings between measures and bounded functions and compensated compactness. *Ann di Matematica Pura ed Appl.* 1983; 135(IV): 293-318.
33. Vese L. A study in the BV space of a denoising-deblurring variational problem. *Appl Math Optim.* 2001;44:131-161.
34. Ivanchuk N, Ivanchuk V. On PDE formulation of the relaxed version of generalized active contour model in anisotropic Sobolev space. *J Optimiz Differ Equat Applicat.* 2024; 32(2):118-136.
35. Aubert G, Kornprobst P. *Mathematical Problems in Image Processing: Partial Differential Equations and the Calculus of Variations*. New York: Springer; 2006: 147.
36. Karami F, Meskine D, Sadik K. A new nonlocal model for the restoration of textured images. *J Appl Anal Comput.* 2019;9(6):2070-2095.
37. Salgado AJ, Wise SM. *Classical Numerical Analysis: A Comprehensive Course*. Cambridge University Press; 2022.
38. Maple C. Geometric design and space planning using the marching squares and marching cube algorithms. In: *2003 International Conference on Geometric Modeling and Graphics*; 2003:90-95.
39. Mantz H, Jacobs K, Mecke K. Utilizing Minkowski functionals for image analysis: a marching square algorithm. *J Stat Mech: Theory Exp.* 2008;12:12015.
40. D'Apice C, Kogut PI, Kupenko O, Manzo R. On variational problem with nonstandard growth functional and its applications to image processing. *J Math Imaging Vis.* 2023;65(3): 472-491.

Ciro D'Apice *obtained the degree cum laude in Mathematics in 1991 and the PhD in Mathematics in 1997 at the University of Naples "Federico II." He is a Full Professor in Mathematical Analysis at Dipartimento di Scienze Aziendali-Management & Innovation Systems (DISA-MIS), University of Salerno. His research interests*

include the following: variational calculus, homogenization and optimal control; complex networks modeling: conservation laws and applications to traffic networks, telecommunication ones, and supply chains, queueing systems and networks; analytical aspects for the temporal and spatial behaviour of solutions of dynamic problems.
https://orcid.org/0000-0003-3194-3063

Umberto De Maio *is an Associate Professor at Dipartimento di Matematica e Applicazioni "R. Caccioppoli", Universitá degli Studi di Napoli Federico II. His research interests include the following: homogenization theory, control theory and asymptotic analysis. He has been the scientific leader of international and national research projects. He was awarded the National Scientific Qualification as a full professor. He has been a Member of several competition committees. He is the coordinator/promoter of Erasmus Exchanges with several international universities. He has been a member of the steering committee of the Double Master's Degree Program in Mathematical Analysis and Modelling. He has been on the organizing committee of several international conferences. He has participated in several national and international conferences. He has taught courses in Mathematical Analysis at several Italian universities. He has been a lecturer in several doctoral courses..*
https://orcid.org/0000-0001-7397-5237

Peter I. Kogut *is a Professor at the Department of Mathematical Analysis and Optimizations, Oles Honchar Dnipro National University, where his teaching focuses on variational methods in mathematical physics, optimal control theory for distributed systems, and nonlinear functional analysis. He received a Ph.D. degree in calculus of variations and optimal control theory in 1989 (Cybernetic Institute of National Academy of Science of Ukraine), and then the scientific degree of Doctor of Sciences in Math and Physics in 1998. In 1998 he was awarded the First Prize of the National Academy of Science for the research in homogenization theory of optimal control problems. He has over 200 journal publications in Mathematical Sciences and 2 books in mathematics that have been published by Birkhauser (2011) and Walter de Gruyter GmbH (2019). His major scientific results cover the different areas of optimization theory, optimal control problems for PDEs, image processing, asymptotic analysis, optimization in partially ordered spaces, and homogenization theory. .*
https://orcid.org/0000-0003-1593-0510

Rosanna Manzo *received a degree cum laude in Mathematics in 1996 and PhD in Information Engineering in 2007 at the University of Salerno. She is an Associate Professor in Mathematical Analysis at the Department of Political and Communication Sciences (DiSPC), University of Salerno. The research activity focuses on the following topics: fluid dynamic models for road networks, telecommunication networks, supply chains and blood flows; optimal control for hybrid systems; variational analysis and optimization in normed spaces; queueing systems and networks.*
https://orcid.org/00000-0002-3891-1825

An International Journal of Optimization and Control: Theories & Applications
(https://accscience.com/journal/ijocta)